sustainability

MDPI

Article

Efficacy of the Simplex-Centroid Method for Optimization of Mixtures of Soil, Ladle Furnace Slag and Fly Ash Applied in Pavement Construction

Mateus Henrique Ribeiro Rodrigues [1], Taciano Oliveira da Silva [1], Heraldo Nunes Pitanga [2], Leonardo Gonçalves Pedroti [1], Klaus Henrique de Paula Rodrigues [1], Emerson Cordeiro Lopes [1] and Gustavo Henrique Nalon [1,*]

[1] Department of Civil Engineering, Federal University of Viçosa, Viçosa 36570-900, Brazil; mateus.ribeiro@ufv.br (M.H.R.R.); taciano.silva@ufv.br (T.O.d.S.); leonardo.pedroti@ufv.br (L.G.P.); klaus@ufv.br (K.H.d.P.R.); emerson.lopes@ufv.br (E.C.L.)

[2] Department of Transportation and Geotechnics, Federal University of Juiz de Fora, Juiz de Fora 36036-330, Brazil; heraldo.pitanga@ufv.br

* Correspondence: gustavo.nalon@ufv.br

Abstract: Integrating industrial wastes into soils to enhance their properties is a potential solution to current waste management challenges. Since the current literature lacks systematic studies on the mechanical performance of mixtures of soil, ladle furnace slag (LFS) and fly ash (FA), this research investigated the chemical stabilization of two different soils (clayey or sandy soil) using a concomitant mix of distinct types of industrial wastes: LFS and FA. A design of experiments (DoE) methodology was employed to systematically generate distinct mixtures for each soil sample, utilizing a simplex-centroid design. The mixtures were subjected to unconfined compressive strength (UCS), California Bearing Ratio (CBR) and resilient modulus (RM) tests. The industrial by-products improved the mechanical properties of the soils, providing UCS, CBR index and RM increases up to 130.5%, 324.4% and 132.6%, respectively. Synergistic and antagonistic effects related to the combination of different wastes were discussed, based on mathematical models with coefficients of determination ranging from 0.760 to 0.998, in addition to response surfaces generated for each response variable. The desirability function was applied to identify the optimal component proportions. The best mixture proportion was 80% soil, 20% LFS and 0% FA, which improved the formation of cemented compounds that contributed to the enhanced mechanical strength. The use of industrial waste for soil stabilization has therefore proven to be technically feasible and environmentally friendly.

Keywords: soil stabilization; ladle furnace slag; fly ash; design of experiments; simplex-centroid network

Citation: Rodrigues, M.H.R.; Silva, T.O.d.; Pitanga, H.N.; Pedroti, L.G.; Rodrigues, K.H.d.P.; Lopes, E.C.; Nalon, G.H. Efficacy of the Simplex-Centroid Method for Optimization of Mixtures of Soil, Ladle Furnace Slag and Fly Ash Applied in Pavement Construction. *Sustainability* **2024**, *16*, 7726. https://doi.org/10.3390/su16177726

Academic Editors: Antonio Caggiano and Shengwen Tang

Received: 8 August 2024
Revised: 2 September 2024
Accepted: 3 September 2024
Published: 5 September 2024

1. Introduction

Ladle furnace slag (LFS) is a steelmaking by-product that originates during the secondary steel refinement in electric arc furnaces (EAF) [1]. Fly ash (FA) consists of fine particles produced by the combustion of pulverized coal in thermal power plants [2]. Given the large generation of these by-products and the potential environmental damage related to their improper disposal in the environment, their management has become a challenge for the industry, which is looking for sustainable and economical applications for these materials [3,4].

An alternative way to reuse LFS and FA is applying both materials as chemical soil stabilizers for highway engineering purposes. This alternative is becoming more attractive with the recent issues regarding the environmental impact of production of Portland cement and lime, which are conventional materials used as chemical soil stabilizers [5]. In this context, several studies have reported the technical suitability of adding individual LFS

or FA to different soil types, aiming to enhance the engineering properties of the natural soils [4,6–11].

The combination of soils, slags and ashes in ternary mixtures has been another sustainable alternative for the road construction industry. However, most studies focused on the study of mixes between soil, ground granulated blast furnace slag and FA, which were recently reviewed by Abdila et al. [12]. In contrast, some previous works investigated the engineering properties of mixtures of soil, LFS and FA [13–17]. These works combined random contents of these two types of by-products and clayey soils and determined the index properties, compaction behavior, permeability, unconfined compressive strength (UCS) and/or California Bearing Ratio (CBR) of the mixtures. However, the CBR swelling (CBR-S) and the resilient modulus (RM) of mixtures of soil, LFS and FA were not investigated in the previous literature. Moreover, the mechanical performance of mixtures of LFS, FA and other types of soils (different from clayey soils) has not yet been investigated in previous papers. The synergistic use of LFS and FA is expected to combine the benefits of the high calcium content of LFS and the high silica and alumina content of FA, improving the development of pozzolanic and self-cementing reactions and enhancing the mechanical properties of the stabilized soil [14]. Moreover, the combination of these industrial by-products offers a cost-effective solution for waste management in industries producing both LFS and FA [17].

In addition, despite the existence of several studies addressing the efficiency of industrial by-products as chemical soil stabilizers, there is no consolidated method focused on the optimization of the design of different types of unconventional chemical stabilizers in mixtures with soils. The absence of systematic criteria to guide the design of waste–soil mixtures is one of the main factors limiting a large-scale application of these types of materials in the road construction industry [18].

An interesting strategy to define mixture proportions that efficiently meet specific design criteria is the design of experiments (DoE). DoE is defined as a branch of applied statistics that deals with planning, conducting, analyzing and interpreting controlled tests to evaluate the factors that control the value of a parameter or group of parameters. DoE is a powerful data collection and analysis tool that can be used in a variety of experimental situations. One of the methods of DoE is the simplex-centroid network. This method allows the elaboration of accurate mathematical models using a reduced number of tests [19]. These mathematical models have the polynomial form presented by Jiao et al. [20] (Equation (1)), which correlates response variables with input variables, allowing the assessment of the influence of an input variable on the response variable, either individually or in combination. Moreover, the optimization of the mathematical model enables the determination of an "optimal" mixture design, in which the response variable is optimized as a function of the input variables [20,21].

$$Y\left(x_1x_2x_3\right) = \beta_1x_1 + \beta_2x_2 + \beta_3x_3 + \beta_{12}x_1x_2 + \beta_{13}x_1x_3 + \beta_{23}x_2x_3 + \beta_{123}x_1x_2x_3 \quad (1)$$

where:

- $Y\left(x_1x_2x_3\right)$ is the response variable in function of components proportions;
- β_i is the calculated regression coefficient;
- x_1, x_2, x_3 are the input variables (percentage of each component in the mixture $(x_1 + x_2 + x_3 = 1)$.

Although the simplex-centroid method has been used in several engineering applications such as the design of ceramic products, mortars and concrete [20–23], there are few studies exploring the efficiency of this method for roadway engineering purposes. Iwański et al. [24] and Onyelowe et al. [25] successfully used the method to optimize the design of cementing compounds used in base course pavements, enhance load-bearing capacity and minimize the expansion of different compounds. However, there is a gap in the technical literature regarding the application of the simplex-centroid method for designing mixtures of different industrial wastes and distinct types of soils. In addition,

there is a notable lack of research on the effects of combining LFS and FA for improving clayey and sandy soils commonly used in pavement structural layers.

To narrow these knowledge gaps, this paper presents the following original contributions to the current state-of-the-art: (i) an evaluation of the technical feasibility of the simplex-centroid method for optimizing the UCS, CBR, CBR-S and RM of ternary soil–LFS–FA mixtures; (ii) the viability of using the simplex-centroid method to design soil–LFS–FA mixtures that meet technical criteria for their application as construction materials of pavements; (iii) the application of the RM as a dosage parameter for the design of soil–waste mixtures; (iv) a pioneering investigation of the synergistic and antagonistic effects of the combined incorporation of LFS and FA on the UCS, CBR, CBR-S and RM of road materials; and (v) a comparison between the effects of LFS and FA on the mechanical performance of soils with different particle size distributions. The consolidation of an efficient method for designing this type of mixture will optimize the reuse of these by-products and provide a technical, environmental and economic option to replace conventional soil stabilizer agents.

Therefore, this work addresses the pressing issue of waste management by proposing an innovative solution that combines LFS and FA as sustainable stabilizers for various types of soils used in pavement construction. By focusing on the beneficial reuse of these materials, this research offers an eco-friendly alternative to traditional soil stabilization methods, reducing the need for landfill disposal and tackling a significant global environmental problem. To systematically implement this waste management strategy, the present study proposes the application of the DoE methodology, utilizing a simplex-centroid design to identify synergistic and antagonistic effects from the combination of LFS and FA. This research also proposes the use of the desirability statistical function to determine the mix proportions that best meet multiple criteria related to UCS, CBR, CBR-S and RM values required for application in pavement construction as base, subbase and subgrade materials. This practical application not only improves the performance of pavement structures but also promotes the sustainable use of waste materials, offering a viable solution to current waste management challenges.

2. Materials

2.1. Soils

Two soil samples collected in Viçosa, Minas Gerais State, Brazil (Soil C and Soil V) were used in this study. One sample is predominantly clayey, referred to as Soil C. The other sample is predominantly sandy, referred to as Soil V. Figure 1 and Table 1 show the particle size distribution for both soil samples, in accordance with NBR 7181 [26]. Table 1 presents the results of soil characterization, according to NBR 6458 [27], NBR 6459 [28] and NBR 7180 [29].

Table 1. Geotechnical characterization and classification of the soil samples.

Parameter	Soil		Parameter	Soil	
	C	V		C	V
Clay ($\Phi \leq 0.002$ mm) (%)	61	5	Specific unit weight (kN/m^3)	28.14	26.57
Silt (0.002 mm < $\Phi \leq 0.06$ mm) (%)	14	24	Liquidity limit (LL)/Plasticity limit (PL)	78/43	36/18
Fine sand (0.06 mm< $\Phi \leq 0.2$ mm) (%)	12	13	Plasticity index (PI) (%)	35	18
Medium sand (0.2 < $\Phi \leq 0.6$ mm) (%)	10	40	USC classification	CH-MH	SC
Coarse sand (0.6 mm < $\Phi \leq 2$ mm) (%)	3	15	TRB classification	A-5-7 (32)	A-2-6
Gravel ($\Phi > 2.0$ mm) (%)	0	3	MCT classification	LA′	NA

Φ: particle diameter.

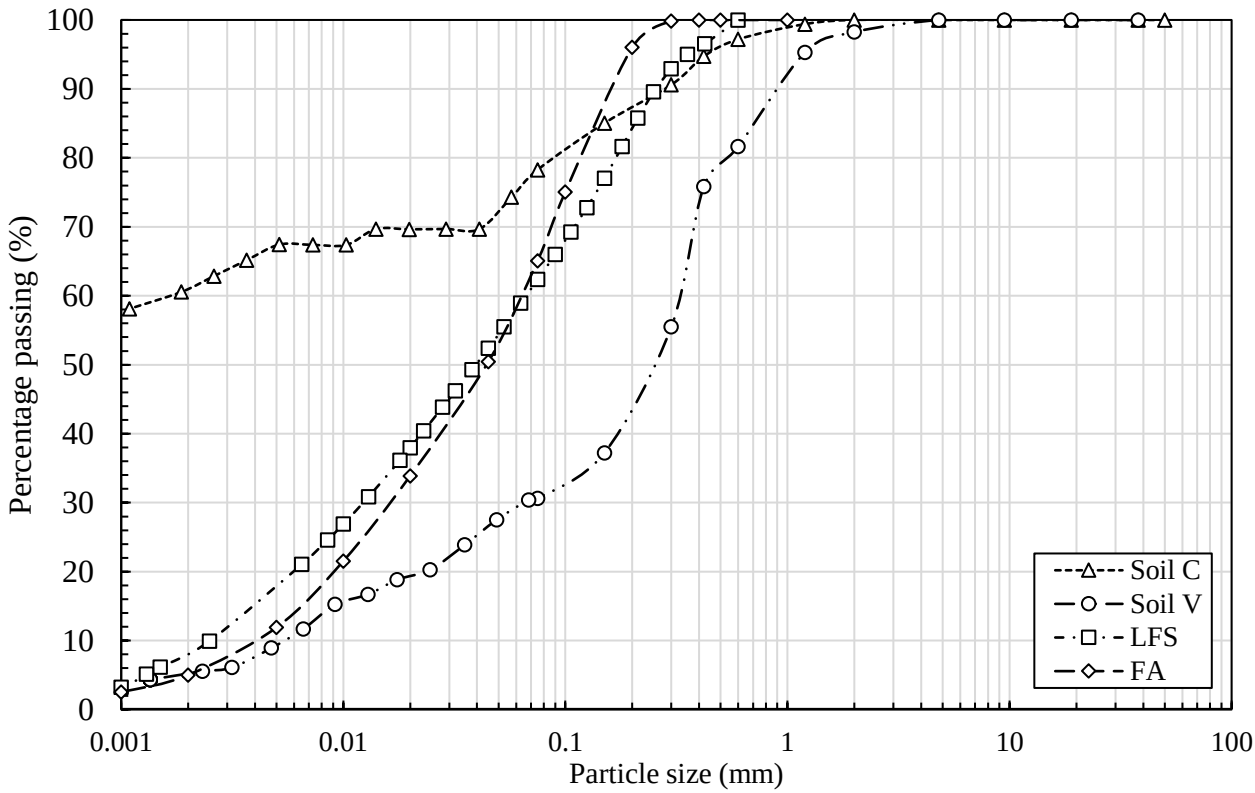

Figure 1. Particle size distribution of soil samples, LFS and FA.

2.2. Ladle Furnace Slag (LFS) and Fly Ash (FA)

The LFS used in this research was collected at the facility of a steel tube manufacturer company, headquartered in Jeceaba, State of Minas Gerais, Brazil. Before being used in this study, the raw LFS was air-dried, milled and sieved to eliminate particles with diameter larger than 0.6 mm (sieve #30) and to increase the LFS-specific surface area in order to reach similar levels considered in other studies dealing with steel slags [30–32]. The FA sample used in this research is classified as type C FA and meets the pozzolanic criteria prescribed in NBR 12653 [33] for pozzolanic materials. Figure 1 shows the LFS and FA particle size distribution determined by laser diffraction according to ISO 13320 [34]. Table 2 presents the results of other laboratory tests performed to physically characterize the LFS and FA.

Table 2. LFS characterization.

Property	LFS	FA	Standard Test Methods
Specific surface area (cm^2/g)	1604.4	1788.24	NBR 16372 [35]
Fineness index (%)	55.8	23.71	NBR 11579 [36]
Specific unit weight (kN/m^3)	29.1	20.8	NBR 16605 [37]

2.3. Chemical Analysis

Table 3 shows the oxide percentages identified in the chemical composition of the materials, which were determined by X-ray fluorescence (XRF) analysis in PANalytical Epsilon3x equipment (Almelo, The Netherlands). The XRF analysis indicated high amounts of SiO_2 and Al_2O_3 in both soil samples and significant Fe_2O_3 content in Soil C sample. Additionally, it was verified that the LFS sample is mainly composed of CaO, SiO_2, Fe_2O_3 and Al_2O_3, while SiO_2 and Al_2O_3 are the main oxides in FA chemical composition.

Table 3. Chemical composition of soils, LFS and FA.

Oxide	Soil C (%)	Soil V (%)	LFS (%)	FA (%)
CaO	0.02	0.07	43.65	1.76
MgO	1.60	1.95	2.43	1.10
SiO_2	33.74	50.19	22.22	61.18
Al_2O_3	30.52	33.63	11.16	24.15
Fe_2O_3	15.52	2.66	17.41	4.26
K_2O	0.08	1.80	0.35	2.84
Na_2O	1.93	3.32	0.97	1.41
SO_3	0.06	0.04	0.71	0.37
Cl	0.33	0.30	0.30	0.21
TiO_2	1.90	0.25	0.71	1.13
LOI *	14.30	5.80	0.09	1.60

* Loss on ignition.

2.4. Mineralogical Analysis

Figure 2 presents the mineralogical phases identified in the samples, based on results of X-ray diffraction (XRD) analyses using a Bruker D8-Discover diffractometer (Billerica, MA, USA) (CuKα radiation, 40 kV, 30 mA, λ = 1.5418 Å, measurement θ–2θ ranging from 5° to 80°, 0.02°/step, 1 s/step). The XRD spectrum of the LFS indicated that portlandite, olivine, calcite and larnite are the main mineralogical phases of this material. The diffractogram of FA revealed mineralogical phases of mullite, wollastonite, quartz and calcite. In the diffractograms of Soil C and V, the main peaks are attributed to quartz and kaolinite, which are common mineralogical phases of soils [38]. The XRD spectrum of Soil C also revealed hematite traces, whereas Soil V also exhibited dolomite, portlandite and biotite signatures.

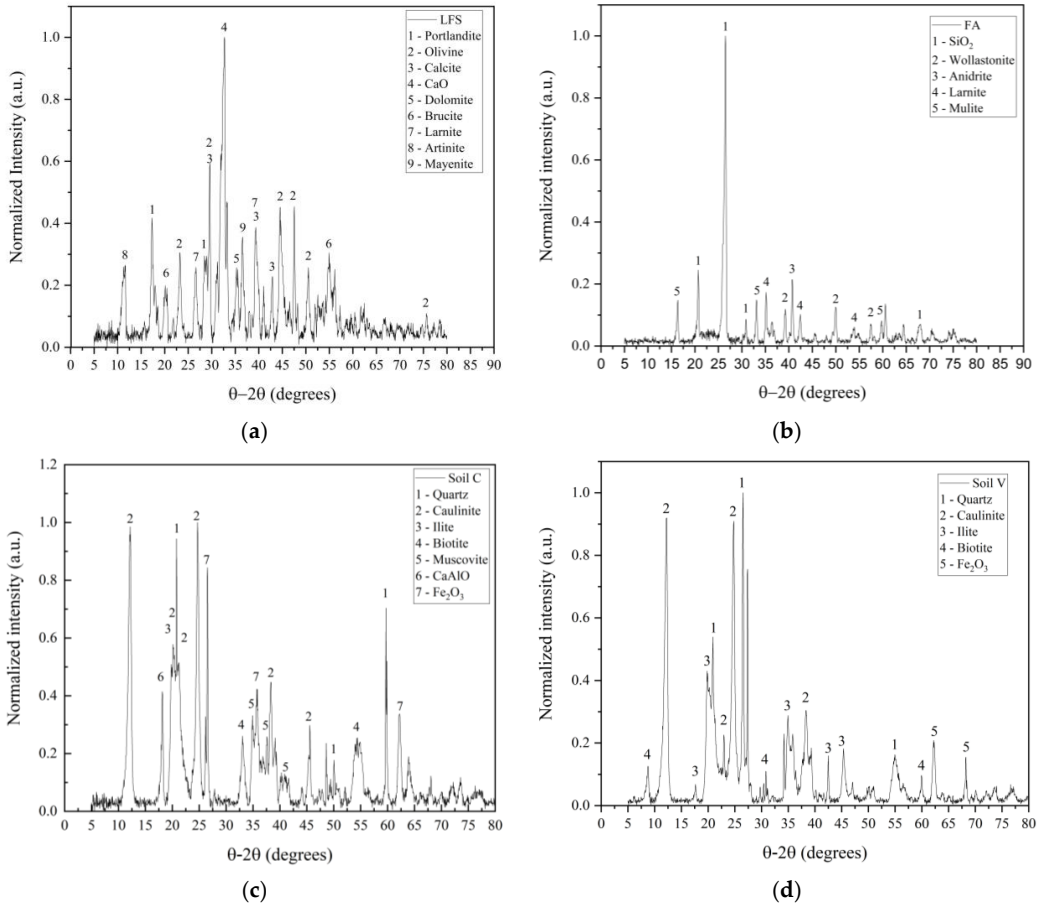

Figure 2. X-ray diffraction patterns of LFS (**a**), FA (**b**), Soil C (**c**) and Soil V (**d**).

2.5. Microstructural Analysis

Figure 3 presents the scanning electron microscopy (SEM) images of the raw materials, obtained with a JEOL JSM-6010LA microscope (Tokyo, Japan) (resolution of 4 nm at 20 kV, magnification of ×8 to ×300,000, and accelerating voltage between 500 V and 20 kV). Figure 3a shows that the LFS has variable geometry, varying from rounded to angular-shaped particles, in addition to rough surfaces and porous aspects. In contrast, Figure 3b indicates that FA particles are mainly hollow spheres with different sizes. The Soil C SEM image [Figure 3c] reveals that this soil presents a compact structure with particle voids filled by smaller-sized minerals. The SEM image of Soil V [Figure 3d] showed a slightly less compacted structure with quartz minerals of different particle sizes.

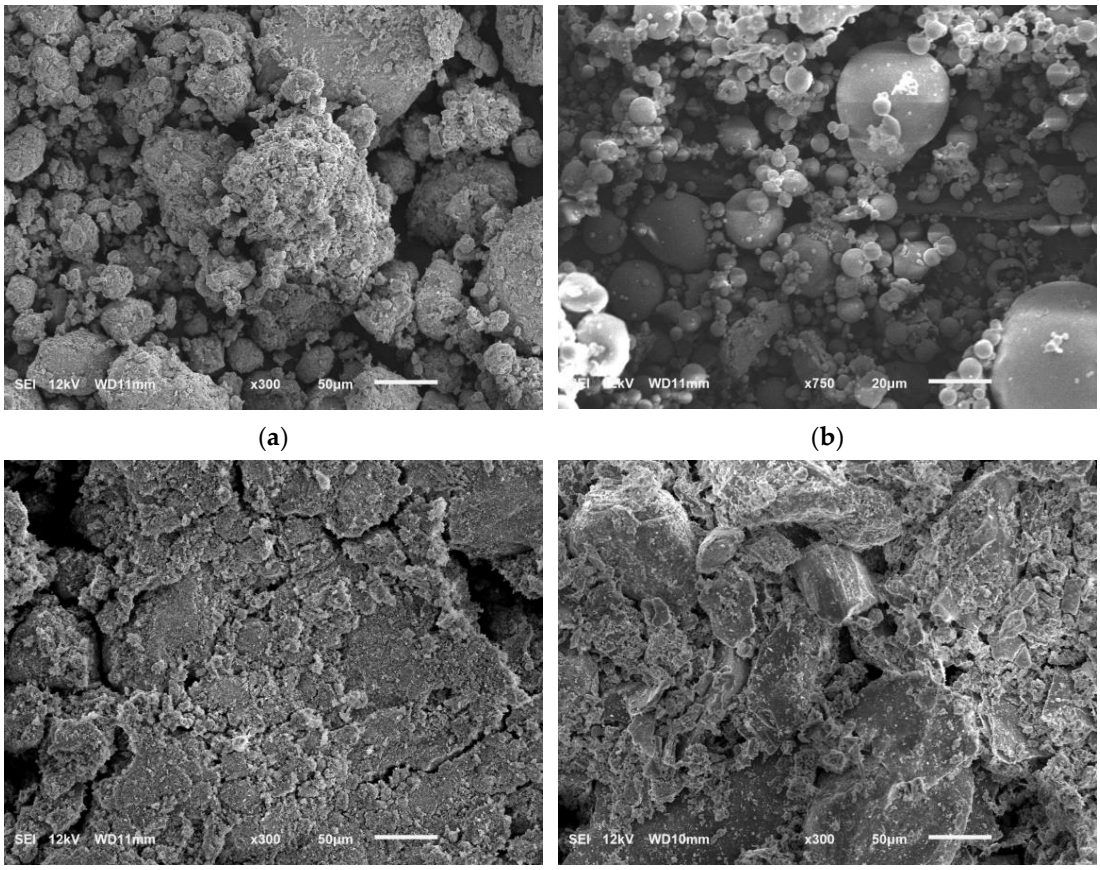

Figure 3. SEM images of LFS (**a**), FA (**b**), Soil C (**c**) and Soil V (**d**).

3. Methods

The methodology used in this research is shown in Figure 4. The flowchart provides a visual representation of the sequential procedures undertaken throughout this study. Each procedure outlined in the flowchart is detailed in the following subsections.

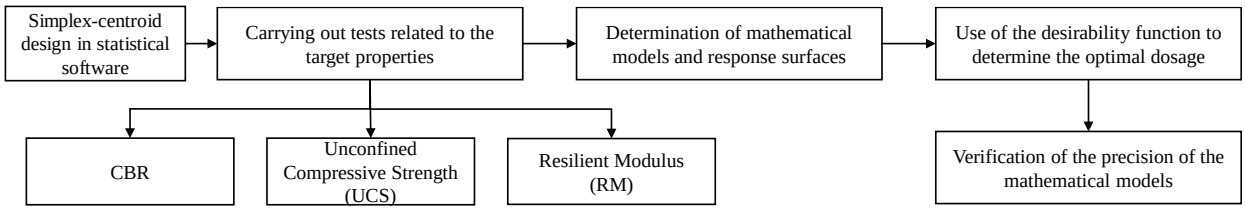

Figure 4. Flowchart of the research processes.

3.1. Design of Experiments

In this study, three materials were used to formulate different experimental mixtures: natural soil (Soil C or Soil V), LFS and FA. The proportions of each mixture composition component were calibrated according to recommendations of industrial by-products contents added to different types of soils in several previous studies [1,15,30,39–41]. LFS contents in the mixture compositions ranged from 5% to 20%, FA contents varied from 0% to 15% and the soil content changed between 80% and 95%, all percentages related to the mixture's total dry mass.

The simplex-centroid ternary diagram shown in Figure 5 illustrates the 7 experimental mixtures (M1 to M7) considered in this study for each soil sample. The proportions of each component in the composition of each experimental mixture are presented in Table 4. The lower and upper limits of the proportions of the individual components were input parameters for the statistical software. Since the simplex-centroid design was used in this work, the variation between the lower and upper limits for all components was the same. The software distributed the experimental points such that there were six equally spaced points on the edges of an equilateral triangle, forming a simplex network. In addition, a central point was included to enhance the accuracy of the final response.

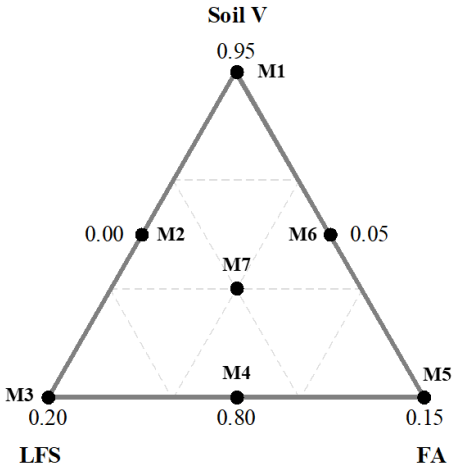

Figure 5. Simplex-centroid ternary diagram.

Table 4. Experimental mixture composition (% in mass).

Material	M1	M2	M3	M4	M5	M6	M7
Soil (%)	95.0	87.5	80.0	80.0	80.0	87.5	85.0
LFS (%)	5.0	12.5	20.0	12.5	5.0	5.0	10.0
FA (%)	0.0	0.0	0.0	7.5	15.0	7.5	5.0

The mixture proportions obtained from the DoE considered only the masses of the materials (soil, LFS and FA) in their dry state. To determine the required water content for producing specimens for mechanical tests, compaction tests were performed at standard Proctor energy, as described below. The optimum moisture content from these tests was then used to define the amount of water needed for each mixture.

3.2. Geomechanical Characterization of Natural Soils and Experimental Mixtures

The pure soil samples (Soil C and Soil V) and the experimental mixtures (M1 to M7) were subjected to laboratory tests to determine (i) UCS (NBR 12025 [42]); (ii) CBR and CBR-S (NBR 9895 [43]) and (iii) RM (ME 134 [44]). These properties were determined using specimens compacted at the optimum moisture content and maximum dry unit weight for the standard Proctor compaction energy. After compaction, all specimens were extracted, wrapped with PVC film and subjected to 7 days of curing in a moist room before

the geomechanical characterization tests. All mechanical properties are directly related to the criteria for the selection of materials for the composition of structural layers of road pavements, as recommended in the technical standard NBR 12253 [45]. The UCS, CBR and CBR-S tests were carried out in triplicate and the results were calculated as the average between all determinations, considering a maximum variation between results of 10%. The RM tests were performed in duplicate.

In the RM tests, the specimens were subjected to dynamic cyclic stress and a static confining stress, using a triaxial pressure chamber and following the procedures prescribed by ME 134 [44]. The strain values were measured using two LVDTs (linear variable displacement transducers) symmetrically positioned within the triaxial cell, aligned with the specimen's central axis. The stress states applied during all RM tests are presented in Table 5. The confining (σ_3) and deviator (σ_d) stresses presented in this table represent the stresses acting on pavement base, subbase and subgrade reinforcements. These values were calculated from the structural analysis of the typical pavement cross-section proposed by Nega and Nikraz [46], considering the stresses acting at the center of each layer and under the wheel of a standard axle [47]. The structural analysis was conducted using the AEMC software [48].

Table 5. Stress state representative of structural layers of flexible pavements.

Layer	σ_3 (MPa)	σ_d (MPa)
Base	0.030	0.160
Subbase	0.010	0.090
Subgrade reinforcement	0.009	0.037

The experimental data obtained from the RM tests were used to develop composite models (Equation (2)), following the recommendations of previous papers and the IS-247 standard [7,49,50], within the context of the MeDiNa (National Pavement Design Method) methodology. Regression analyses were performed to develop a mathematical model (k_1, k_2 and k_3 were the regression coefficients) that predicts the material's deformational characteristics, providing an RM value for design purposes.

$$RM = k_1 \times (\sigma_3)^{k_2} \times (\sigma_d)^{k_3} \quad (2)$$

where:

- RM is the resilient modulus (MPa);
- σ_3 is the confining stress (MPa);
- σ_d is the deviator stress (MPa);
- k_1, k_2, k_3 are the regression model coefficients.

3.3. Mathematical Models and Response Surfaces

The UCS, CBR, E-CRB and RM responses of each experimental mixture (M1 to M7) allowed the determination of polynomial models that correlate each property to the mixture component contents. These models were estimated using statistical analysis software for development of stepwise regression and analysis of variance (ANOVA), considering a significance level of 5% and a confidence limit of 95%. These mathematical models provided response surfaces that graphically described the variation of the experimental response as a function of the mass percentage of each mixture component.

3.4. Simplex-Centroid Method Efficiency and Mixture Design Optimization

The efficiency of the simplex-centroid method in predicting the mechanical behavior of soil–LFS–FA mixtures was evaluated by comparing some experimental results with data estimated using mathematical models. The mixture design optimization was performed using the desirability function. This function provides desirability values ranging from 0 to

1 for each mixture, where 1 represents that the mixture fully met the defined design criteria, and 0 indicates that the design criteria were not met.

The soil–LFS–FA mixture design optimization was performed, aiming to reach a mix composition that better met the different criteria established for UCS, CBR, CBR-S and RM, allowing its practical application in structural layers of pavements. Therefore, the mixture with higher desirability value corresponded to the mixture whose design was optimized. To evaluate each mixture's suitability as a base, subbase and subgrade construction material, the mechanical and swelling criteria presented in Table 6 were considered.

Table 6. Criteria for design optimization of the experimental mixtures.

Base Course			
Property	Soil C	Soil V	Reference
UCS (kPa)	Min. 690		AASHTO [51] and Ardah et al. [52]
CBR (%)	Min. 60		DNIT [53]
CBR-S (%)	Max. 0.5		
RM (MPa)	Min. 82.74	Min. 165.47	AASHTO [54]
Subbase Course			
Property	Soil C	Soil V	Reference
UCS (kPa)	Min. 690		AASHTO [51] and Ardah, Chen and Abu-Farsakh [52]
CBR (%)	Min. 20		DNIT [53]
CBR-S (%)	Max. 1.0		
RM (MPa)	Min. 82.74	Min. 165.47	AASHTO [54]
Subgrade Reinforcement Course			
Property	Soil C	Soil V	Reference
UCS (kPa)	Min. 345		Ardah, Chen and Abu-Farsakh [52]
CBR (%)	Min. 2		DNIT [53]
CBR-S (%)	Max. 1.0		
RM (MPa)	Min. 68.95	Min. 68.95	AASHTO [54]

4. Results and Discussion

4.1. Experimental Response, Response Surfaces and Mathematical Models

Table 7 shows the UCS values of the natural soils (M0) and each tested mixture (M1 to M7). These values were used to derive the prediction equations for UCS of mixtures produced with Soil C and Soil V (Equations (3) and (4), respectively). The UCS contour surfaces are shown in Figure 6. The parameters S, L and F correspond to the percentages of the contents of soil, LFS and FA, respectively.

$$UCS = 166 \times S + 1573 \times L + 2139 \times F - 18733 \times L \times F;\ R^2 = 0.8752 \quad (3)$$

$$UCS = 109.6 \times S + 396.6 \times L + 382.1 \times F;\ R^2 = 0.8897 \quad (4)$$

The partial replacement of natural soils with by-products provided significant increases in UCS. The highest UCS increases observed in specimens produced with Soils C and V were observed in M3 and M5 mixtures, respectively. In the M3 mixture, the replacement of 20% of Soil C by LFS provided a percentage UCS increase of 130.5%. In the M4 mixture, the replacement of 5% of Soil V by LFS and 15% of Soil V by FA provided a percentage UCS increase of about 63.0%.

Table 7. UCS (kPa) of natural soils and experimental mixtures.

Material	**M0**	**M1**	**M2**	**M3**	**M4**	**M5**	**M6**	**M7**
Soil C	203.7	243.2	293.7	469.6	309.0	377.2	339.5	322.0
Soil V	102.1	117.2	150.6	165.5	161.7	166.4	148.5	162.1

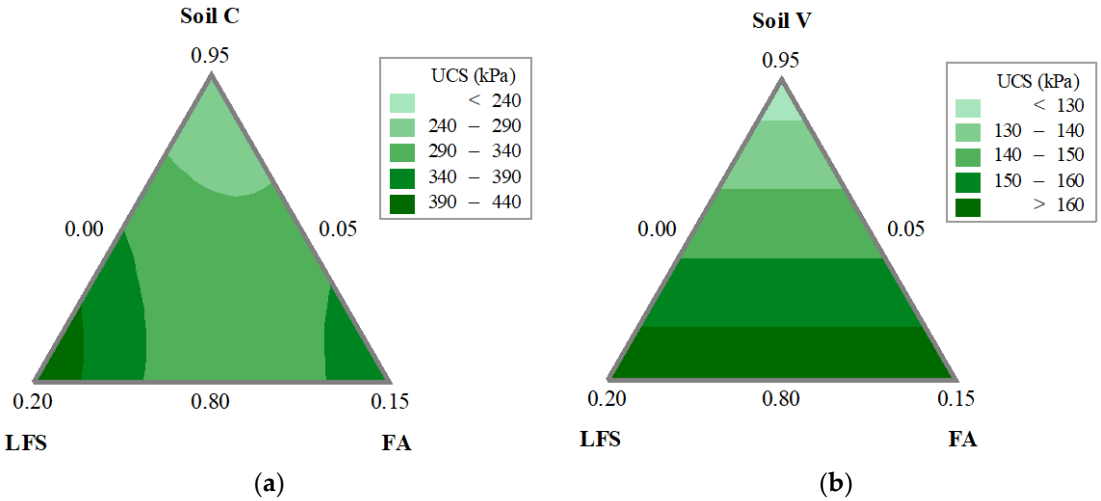

Figure 6. UCS contour surfaces of Soil C (**a**) and Soil V (**b**) experimental mixtures.

The maximum percentage UCS increases observed in the present study were higher than those reported in previous studies. For example, Fathonah, Intari, Mina, Kusuma and Mahfudoh [13] observed that the best UCS improvement was approximately 50% (after a curing period of 7 days), which was obtained for a mixture of 70% of clayey soil, 20% of FA and 10% of LFS. The maximum UCS increase reported by Rajakumaran [16] was about 7.3%, in a mixture of 90% of clayey soil, 4% of LFS and 6% of FA (the curing period was not mentioned in this paper).

Table 8 presents the CBR values obtained from the laboratory tests of natural soils (M0) and experimental mixtures (M1 to M7). The mathematical descriptive models representing the CBR of mixtures containing Soil C and Soil V were presented in Equations (5) and (6), respectively. The response surfaces related to this mechanical property are presented in Figure 7.

$$CBR = 17.36 \times S + 96.35 \times L - 41.44 \times F;\ R^2 = 0.7792 \quad (5)$$

$$CBR = 7 \times S + 145 \times L + 92 \times F - 1583 \times S \times L \times F;\ R^2 = 0.9987 \quad (6)$$

Table 8. CBR (%) of the soil samples and experimental mixtures.

Mixture	M0	M1	M2	M3	M4	M5	M6	M7
Soil C	11.2	17.8	29.0	32.6	18.2	12.1	18.2	28.4
Soil V	8.2	14.1	23.9	34.8	18.6	17.2	14.9	18.7

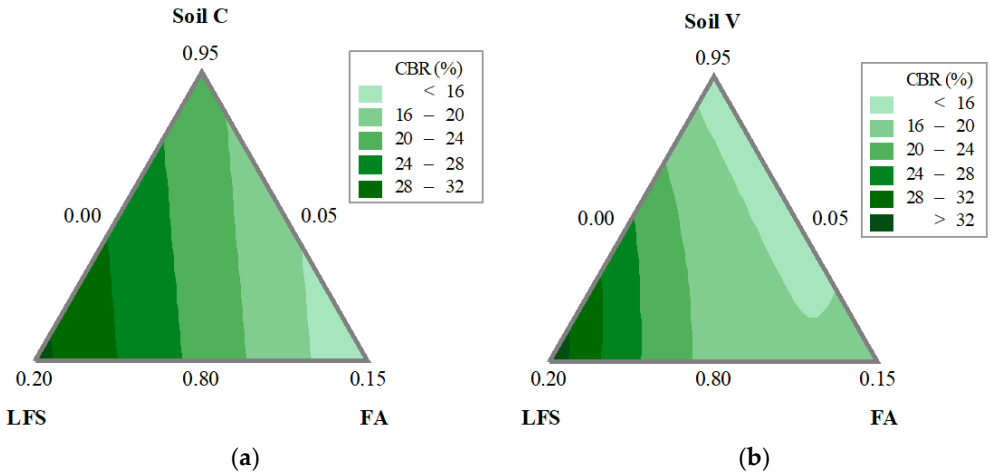

Figure 7. CBR contour surfaces of Soil C (**a**) and Soil V (**b**) experimental mixtures.

The CBR index of the soils was significantly improved by the addition of both by-product types. For both soils, the greatest improvements in CBR index were verified in M3 mixtures. In this case, the replacement of 20% of Soil C and V by LFS provided percentage CBR index increases of 191.1% and 324.4%, respectively. All percentage CBR improvements observed in this study were lower than the maximum CBR increases provided by the LFS and FA analyzed by Mina, Kusuma and Ulfah [14]. After a 7-day curing period, they reported a maximum CBR increase of 642% when 20% of FA and 20% of LFS were added to clayey soils. For a 7-day curing period, Soyonar, Fırat, Yilmaz and Okur [17] observed that the CBR index of mixtures of 80% of LFS, 15% of FA and 5% of clayey soil was 51.4% higher than the CBR index of their reference clay–slag mixture.

Table 9 presents the results for CBR-S values obtained from the laboratory tests of natural soils (M0) and experimental mixtures (M1 to M7). The mathematical descriptive models representing the CBR-S of mixtures produced with Soil C and Soil V are presented in Equations (7) and (8), respectively. The response surfaces obtained from the CBR-S results are presented in Figure 8.

$$CBR - S = 0.1697 \times S + 0.6845 \times L - 0.397 \times F + 70.3849 \times S \times L \times F;\ R^2 = 0.9063 \quad (7)$$

$$CBR - S = 0.849 \times S - 1.551 \times L - 1.737 \times F;\ R^2 = 0.2281 \quad (8)$$

Table 9. CBR-S (%) of the soil samples and the experimental mixtures.

Mixture	M0	M1	M2	M3	M4	M5	M6	M7
Soil C	0.7	0.2	0.3	0.3	0.8	0.5	0.5	0.4
Soil V	0.3	0.8	0.5	0.2	0.5	0.3	0.2	1.0

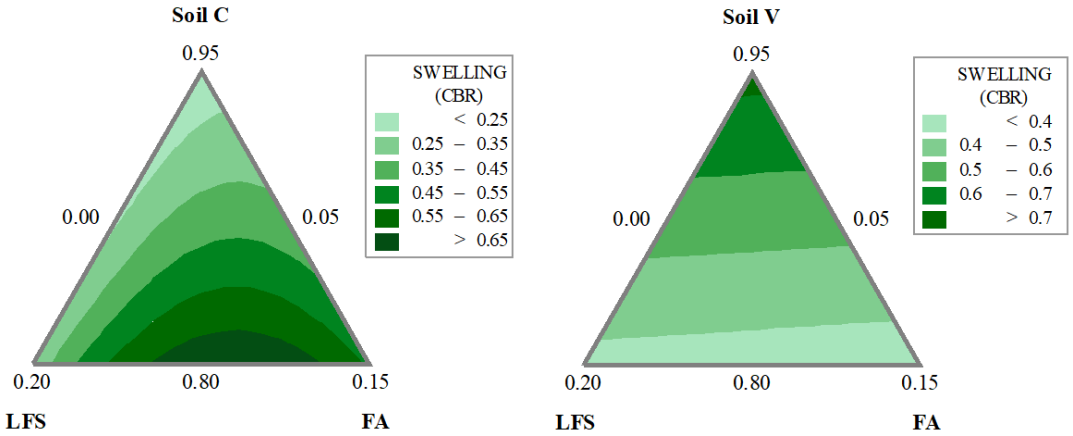

Figure 8. CBR-S contour surfaces of Soil C (**a**) and Soil V (**b**) experimental mixtures.

Significant data scatter was observed in CBR-S results, which compromised the predictive ability of the developed mathematical models, as discussed in the next subsections. The average CBR-S values of all mixtures with Soil C were lower than the average CBR-S of the natural soil, except for mixture M4. In contrast, the average CBR-S values of all mixtures with Soil V were higher than the CBR-S of the natural soil, except for mixtures M3 and M6. When Soil C was used, the highest swelling reduction was provided by the replacement of 5% of Soil C by LFS (mixture M1). When Soil V was used, the highest swelling reductions were provided by the replacement of 20% of Soil V by LFS (mixture M3) or replacement of 5% of Soil V by LFS and 7.5% of Soil V by FA (mixture M6). Despite the natural variability of the experimental data, the incorporation of by-products into both soil types did not result in significant increases in soil expansion, which is a promising result to enable their application in road construction.

Table 10 displays the coefficients of the RM models of each experimental mixture (M1 to M7) and natural soils (M0). These values were obtained from the experimental data considering the stress states that are representative of each pavement structural layer considered in this study.

Table 10. RM values of soil and experimental mixtures.

Experimental Mixture		RM Model Coefficient			Coefficient of Determination (R^2)	RM Obtained from Experimental Data (MPa)		
		k_1	k_2	k_3		Base	Subbase	Subgrade Reinforcement
Soil C	M0	423.609	−0.016	−0.634	0.729	28.32	29.63	35.81
	M1	42.041	0.173	−0.139	0.685	29.57	26.49	29.43
	M2	64.314	0.237	−0.228	0.939	42.54	37.39	44.66
	M3	70.111	0.153	−0.160	0.732	54.97	50.95	57.79
	M4	45.12	0.139	−0.179	0.819	38.47	36.61	42.30
	M5	51.607	0.241	−0.160	0.728	29.72	25.01	28.10
	M6	34.038	0.096	−0.160	0.728	32.59	32.16	36.70
	M7	62.018	0.164	−0.151	0.751	46.02	41.92	47.12
Soil V	M0	146.541	0.563	−0.026	0.690	21.34	11.67	11.26
	M1	57.391	0.308	−0.249	0.731	30.76	25.31	30.57
	M2	158.408	0.305	0.129	0.921	42.92	28.50	24.61
	M3	311.022	0.401	0.246	0.972	48.57	27.14	20.90
	M4	107.273	0.356	−0.114	0.686	37.94	27.40	29.20
	M5	108.962	0.327	−0.017	0.938	35.71	25.18	24.70
	M6	89.001	0.294	−0.008	0.941	32.21	23.43	22.88
	M7	118.068	0.448	−0.253	0.729	39.02	27.59	32.95

Equations (9)–(11) show the mathematical models that describe the RM of mixtures containing Soil C, considering the state stress representative of the base, subbase and subgrade layer, respectively. Equations (12)–(14) exhibit the models obtained for the RM of mixtures containing Soil V, considering the state stress representative of the base, subbase and subgrade layer, respectively. The response surfaces that graphically illustrate these equations are shown in Figures 9–11.

$$RM = 24.51 \times S + 175.66 \times L + 14.46 \times F;\ R^2 = 0.8604 \quad (9)$$

$$RM = 18 \times S + 183 \times L - 1191 \times F + 1499 \times S \times F;\ R^2 = 0.9511 \quad (10)$$

$$RM = 20 \times S + 212 \times L - 1339 \times F + 1682 \times S \times F;\ R^2 = 0.9670 \quad (11)$$

$$RM = 26.48 \times S + 136.75 \times L + 39.60 \times F;\ R^2 = 0.8952 \quad (12)$$

$$RM = 24.51 \times S + 44.86 \times L + 20.88 \times F;\ R^2 = 0.4980 \quad (13)$$

$$RM = 32.7 \times S - 25.85 \times L - 89.64 \times F + 1588.89 \times L \times F;\ R^2 = 0.6700 \quad (14)$$

Considering the lack of prior investigations into the RM of soil–LFS–FA mixtures, the RM dataset obtained in the present research complements the current knowledge on the resilient behavior of these mixtures, considering their application to different pavement structural layers. Regardless of the structural layer, the RM of both types of soils was improved by the addition of LFS and/or FA. Previous research [55] also verified that waste-based pavement materials can exhibit improved stiffness compared to conventional pavements, enabling them to withstand high stresses with less deformation. For both soil types, the best RM improvements were observed in M3 mixtures. In this situation, the replacement of 20% of Soil C and V by LFS provided percentage RM increases up to 94.1% and 132.6%, respectively.

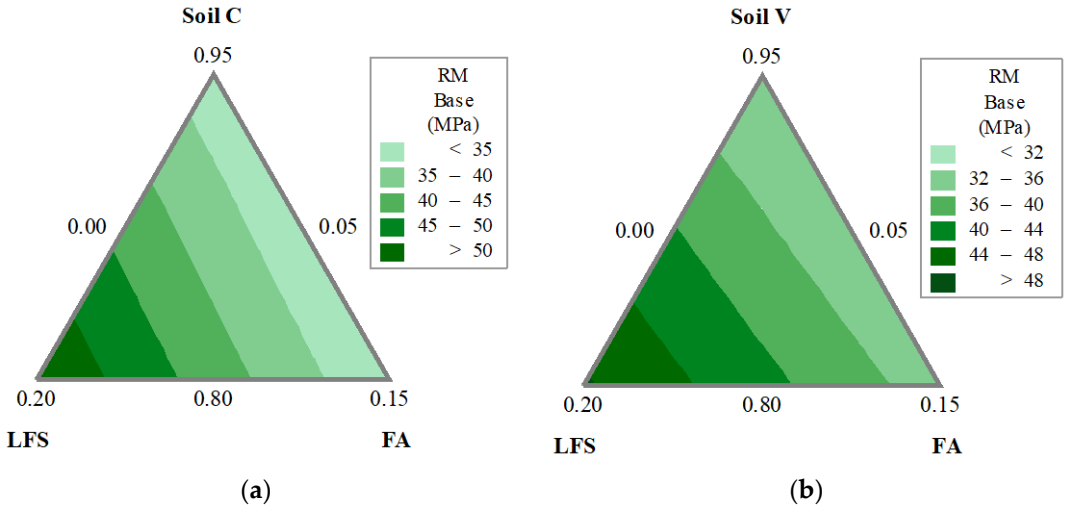

(**a**) (**b**)

Figure 9. RM response surfaces of the experimental mixtures prepared with Soil C (**a**) and Soil V (**b**), considering the state stress representative of the base course of flexible pavements.

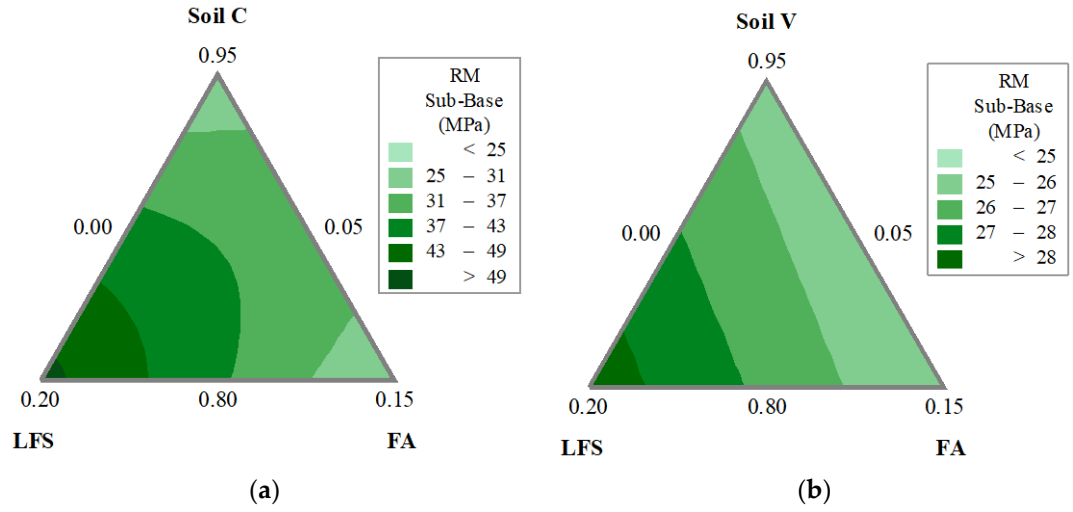

(**a**) (**b**)

Figure 10. RM response surfaces of the experimental mixtures prepared with Soil C (**a**) and Soil V (**b**), considering the state stress representative of the subbase course of flexible pavements.

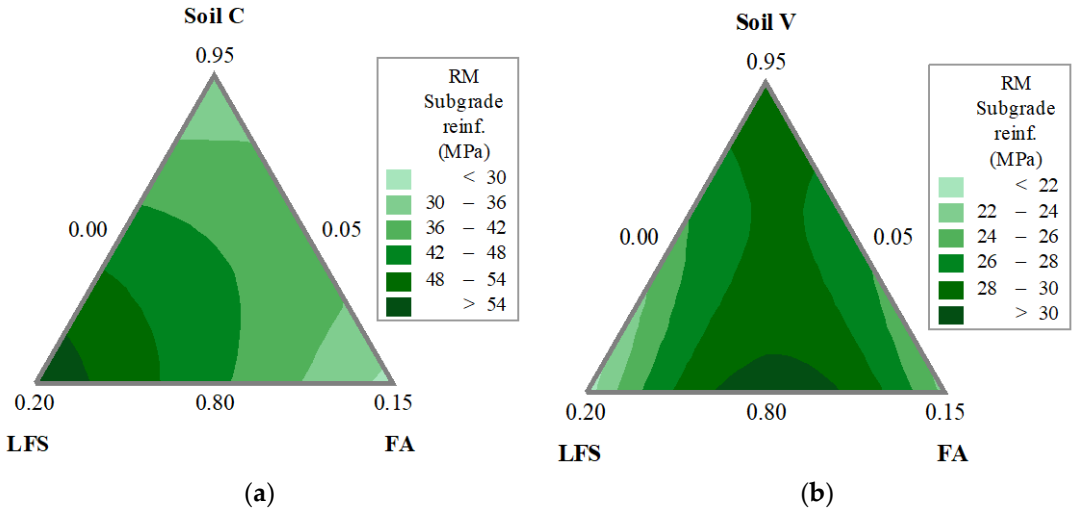

(**a**) (**b**)

Figure 11. RM response surfaces of the experimental mixtures prepared with Soil C (**a**) and Soil V (**b**), considering the state stress representative of the subgrade reinforcement layer of flexible pavements.

According to previous research [3,6,15,56–58], the development of cementitious and/or pozzolanic reactions due to the incorporation of LFS or FA leads to the formation of calcium aluminates and calcium silicates that improve the filler effect and the connections between soil aggregates, which explains the improvements in mechanical performance described in the present section. Previous work [58] also reported that rod-like crystals are formed after the carbonation of steel slag, which has a binding effect and is also advantageous for strength development. The present study introduced a comparative analysis of the effects of the addition of LFS and FA on different types of soils. According to the results verified in most of the mixtures investigated in this work, it was possible to note that the percentage increases in UCS, CBR and RM due to the addition of LFS and FA were higher in Soil V (sandy soil) than in Soil C (clayey soil). This can be attributed to stronger contact bridges between the surface of particles of granular soils (Soil V) provided by LFS and FA. Such strong anchoring mechanisms between particles of Soil C were not possible due to the small size of the clay particles [7,59]. Consequently, the benefits provided by LFS and FA were more pronounced in the sandy soil than in the clayey soil.

In the present work, UCS, CBR, CBR-S and RM were determined under controlled laboratory conditions. However, it is essential to consider that different variables in real-world environments can impact the long-term performance of the soil–waste mixtures. Our research group recently performed an environmental characterization of the LFS [60] and FA [6] used in this study, based on leaching and solubilization tests [61]. These tests classified the wastes as Class II A solid wastes, indicating that they are non-hazardous and non-inert. Nevertheless, future studies should conduct in-situ tests alongside laboratory assessments, as previous research [62] has revealed several challenges in field trials, such as rutting issues and layer settling in mixtures containing high waste dosages. These in-situ evaluations can offer valuable insights into the performance of these materials under actual environmental conditions and traffic loads, helping to identify and address potential issues that may not be detected through laboratory testing alone.

4.2. Response Surfaces and Mathematical Models Evaluation

Regarding the Soil C mixtures, Figures 6a and 7a suggest that the mixtures with the highest amount of LFS (M3) exhibited the greatest UCS and CBR values. This fact indicates that FA addition had less influence on UCS and CBR than the LFS addition. This hypothesis is confirmed by analyzing the model coefficients obtained for these properties (Equations (3) and (5)). Once β_1 and β_2 are positive in both models, it is expected that the UCS and CBR values increase with increases in LFS content. Regarding the effects of FA on the UCS and CBR, the negative β_{23} coefficient (Equation (3)) indicated that the combination between LFS and FA had a negative impact on those properties, so the influence of an increasing FA content in the mixture was represented by a negative β_3 coefficient (Equation (5)).

Figure 9a indicated that the highest swelling values were verified in the lower central portion of the diagram (M4), the region in which the mixtures had the lowest soil contents and highest dosages of by-products in their composition. In addition, the coefficient β_{123} (Equation (7)) was greater than the other model coefficients. These findings indicate that the combination of the three components contributed to increase the swelling of the mixtures.

Regarding the RM values of the Soil C mixtures [Figures 9a, 10a and 11a], it is noticed that the greatest RM values were obtained for the mixtures located at the left bottom corner of the diagram, regardless of the stress state. This behavior is an indication that LFS had a beneficial effect on the RM of the mixtures. This hypothesis is reinforced by the evaluation of Equations (9)–(11). In most equations the β_2 coefficient is positive, while β_3 is negative, indicating that the LFS addition had positive impacts, while the FA addition had detrimental effects on the RM of the mixtures, which is pretty similar to the general behavior verified in the response surfaces. In addition, the β_{13} coefficient of Equations (10) and (11) shows that the interaction between Soil C and FA contributes positively to increasing the

mixtures' RM only for stress state levels corresponding to the load acting on subbase and subgrade reinforcement layers.

Even though some coefficients of the proposed descriptive models (Equations (3), (5), (7) and (9)–(11)) did not show statistical relevance in some statistical analyses, it is important to note that the models presented R^2 values ranging between 0.7792 and 0.9063, which indicates good correlation between the experimental data and the proposed models.

Regarding the Soil V mixtures, the mixtures M3, M4 and M5 located at the lower central edge of the diagram of Figure 6b presented the highest UCS values. This finding indicates that the LFS and FA addition contributed to an increase in the UCS values. This hypothesis was confirmed by the coefficients β_1, β_2 and β_3 (Equation (4)). Since these coefficients were positive and had similar magnitude, it is possible to infer that the addition of LFS and FA had a positive and quantitatively similar impact on the UCS of the experimental mixtures.

Figure 7b indicates that mixtures with higher CBR values are located at the left bottom corner of the diagram. A similar trend is observed for RM values associated with stress states acting on base and subbase layers of flexible pavements [Figures 9b and 10b]. In addition, β_2 and β_3 coefficients of the respective models are positive (Equations (6), (12) and (13)). These observations indicated that LFS had greater influence on CBR and base and subbase RM values compared to the influence of FA on these mechanical properties. Regarding the CBR descriptive equation of soil V mixtures (Equation (6)), it is also noteworthy that the β_{123} coefficient was negative and statistically significant, which indicates that the combination of all three components had a negative impact on the CBR of the mixtures.

Concerning the RM values associated with the stress state representative of subgrade reinforcement, it was verified that the highest RM values are located at the lower central portion of the diagram [Figure 11b]. In this case, the model coefficients presented in Equation (14) indicated that the LFS and FA addition had a negative influence on the RM values, since β_2 and β_3 were negative. However, Equation (14) suggested that the interaction between LFS and FA (coefficient β_{23}) positively influenced the RM of the mixtures, which justifies the behavior indicated in the diagram presented in Figure 11b.

Regarding the CBR-S of Soil V mixtures [Figure 8b], it was observed that the highest values were found in the upper middle portion of the diagram. According to Equation (8), both β_2 and β_3 coefficients are negative, which indicates that LFS and FA addition tended to reduce the CBR-S of the experimental mixtures when keeping the other independent variables constant.

It is important to notice that the mathematical model presented in Equation (8) did not show good data correlation, resulting in an R^2 equal to 0.2281, which is significantly inferior to the R^2 obtained for the mathematical models that represent all of the other properties evaluated in this study. Since this CBR-S equation (Equation (8)) did not show a good fit to the experimental data, it was not taken as representative for predicting the CBR-S of the mixtures. Therefore, the CBR-S criteria were not taken into consideration during the optimization design process developed for the Soil V mixtures in the next subsections.

Although some coefficients of the proposed models presented in Equations (4), (6) and (12)–(14) did not show statistical significance in some analyses, the mathematical models still presented reasonable correlation with the experimental data since R^2 values between 0.4980 and 0.9987 were obtained. For UCS and CBR values, the models presented an excellent fit to the experimental data, with R^2 values greater than 0.8897. RM models of mixtures prepared with Soil V for subbase and subgrade reinforcement layers (R^2 = 0.4980 and R^2 = 0.6700, respectively) provided a poorer fit to the experimental data compared to the model obtained for the RM of base layers (R^2 = 0.8952). Despite this, the models referring to the subbase and subgrade reinforcement layers were reasonably sufficient to represent the RM behavior of the mixtures and carry out the optimization process.

4.3. Simplex-Centroid Method Efficiency Evaluation

Tables 11 and 12 show the average variation between the experimental results and each property estimated by the developed mathematical models. Analyses of the UCS and

CBR results of Soil C mixtures indicated that, except for mixtures M2, M1, M4 and M7, average variations between obtained and predicted data were lower than 7.1%. The high variations observed in some mixtures are probably related to variations inherent to the specimen's compaction process and to the heterogeneity of the materials. Although a few high-magnitude variations (~20%) were verified, the average variation was around 12.1%, indicating that the mathematical models can provide a good estimate of the UCS and CBR values of the experimental mixtures.

Table 11. Simplex-centroid effectiveness evaluation in predicting the UCS, CBR and CBR-S of the experimental mixtures.

UCS (kPa)						
Mixture	Soil C			Soil V		
	Experimental	Model	Variation	Experimental	Model	Variation
M1	243.2	236.4	2.8%	117.2	123.9	−5.8%
M2	293.7	341.9	−16.4%	150.6	145.9	3.1%
M3	469.6	447.4	4.7%	165.5	167.9	−1.4%
M4	309.0	314.2	−1.7%	161.7	167.8	−3.8%
M5	377.2	391.8	−3.9%	166.4	167.7	−0.8%
M6	339.5	314.1	7.5%	148.5	145.8	1.8%
M7	322.0	311.7	3.2%	162.1	153.2	5.5%
	Absolute mean variation		5.7%	Absolute mean variation		3.2%
CBR (%)						
Mixture	Soil C			Soil V		
	Experimental	Model	Variation	Experimental	Model	Variation
M1	17.8	21.3	−20.0%	14.1	13.9	1.4%
M2	29.0	27.2	6.0%	23.9	24.3	−1.5%
M3	32.6	33.2	−1.9%	34.8	34.6	0.6%
M4	18.2	22.8	−25.1%	18.6	18.8	−0.8%
M5	12.1	12.5	−3.2%	17.2	17.2	0.3%
M6	18.2	16.9	7.1%	14.9	15.1	−1.2%
M7	28.4	22.3	21.5%	18.7	18.3	2.0%
	Absolute mean variation		12.1%	Absolute mean variation		1.1%
CBR-S (%)						
Mixture	Soil C			Soil V		
	Experimental	Model	Variation	Experimental	Model	Variation
M1	0.2	0.2	−22.2%	0.8	0.7	2.8%
M2	0.3	0.2	16.4%	0.5	0.5	−3.6%
M3	0.3	0.3	−4.9%	0.2	0.4	−130.6%
M4	0.8	0.7	5.3%	0.5	0.4	26.0%
M5	0.5	0.5	−6.5%	0.3	0.3	−17.6%
M6	0.5	0.4	18.3%	0.2	0.5	−167.5%
M7	0.4	0.5	−23.0%	1.0	0.5	49.5%
	Absolute mean variation		13.8%	Absolute mean variation		56.8%

Regarding the simplex-centroid efficiency in predicting the UCS and CBR of Soil V mixtures, variations lower than 6.00% were verified between estimated and obtained UCS and CBR values, which highlights the method effectiveness in predicting these properties for Soil V mixtures.

Table 12. Simplex-centroid effectiveness evaluation in predicting the resilient modulus (RM) of the experimental mixtures.

RM (MPa)—Soil C									
Mixture	Base			Subbase			Subgrade reinforcement		
	Experimental	Model	Variation	Experimental	Model	Variation	Experimental	Model	Variation
M1	29.57	32.07	−8.4%	26.49	26.25	0.9%	29.43	29.60	−0.6%
M2	42.54	43.40	−2.0%	37.39	38.63	−3.3%	44.66	44.00	1.5%
M3	54.97	54.74	0.4%	50.95	51.00	−0.1%	57.79	58.40	−1.1%
M4	38.47	42.65	−10.9%	36.61	37.89	−3.5%	42.30	43.00	−1.6%
M5	29.72	30.56	−2.8%	25.01	24.78	0.9%	28.10	27.59	1.8%
M6	32.59	31.31	3.9%	32.16	33.95	−5.6%	36.70	38.06	−3.7%
M7	46.02	39.12	15.0%	41.92	37.76	9.9%	47.12	42.74	9.3%
	Mean absolute variation		6.2%	Mean absolute variation		3.5%	Mean absolute variation		2.8%
RM (MPa)—Soil V									
Mixture	Base			Subbase			Subgrade reinforcement		
	Experimental	Model	Variation	Experimental	Model	Variation	Experimental	Model	Variation
M1	30.76	32.0	−4.0%	25.31	25.53	−0.9%	30.57	29.77	2.6%
M2	42.92	40.3	6.2%	28.50	27.05	5.1%	24.61	25.38	−3.1%
M3	48.57	48.5	0.1%	27.14	28.58	−5.3%	20.90	20.99	−0.4%
M4	37.94	41.2	−8.7%	27.40	26.78	2.2%	29.20	31.10	−6.5%
M5	35.71	34.0	4.9%	25.18	24.98	0.8%	24.70	23.34	5.5%
M6	32.21	33.0	−2.4%	23.43	25.26	−7.8%	22.88	26.56	−16.1%
M7	39.02	38.2	2.2%	27.59	26.36	4.4%	32.95	28.67	13.0%
	Mean absolute variation		4.1%	Mean absolute variation		3.8%	Mean absolute variation		6.7%

On the other hand, a high variation was observed in the CBR-S values. Therefore, it was observed that the method was not efficient in describing this property, as most mixtures prepared with Soil C presented variation results higher than 15%. For Soil V mixtures, the variation between experimental and predicted data for CBR-S was even greater (sometimes higher than 100%) than the variation verified for Soil C mixtures, which evidenced the inefficiency of this method in predicting the mixture CBR-S response. Such variations are attributed to the poor correlation between the experimental data and the predictions provided by the developed mathematical models.

The evaluation of the RM results indicated that the maximum variation between predicted and obtained RM values was 15% for the Soil C mixtures, and 16.1% for the Soil V mixtures. Despite these variations, the absolute mean variation between the RM values was around 2.8% and 6.7% for Soil C and Soil V mixtures, respectively, demonstrating the effectiveness of the method in predicting the RM values of the experimental mixtures prepared with both soil types.

4.4. Mixtures Design Optimization for Pavement Construction

Aiming to apply the soil–LFS–FA mixtures in structural layers of asphalt pavements, response surfaces were obtained with a design optimization process of Soil C and V mixtures, as presented in Figures 12–14. The CBR-S criterion was not considered during the optimization process of Soil V mixtures since the mathematical model developed for this property presented a low R^2 value.

In mixtures prepared with Soil C, the greatest desirability values were observed for mixtures located at the left bottom corner of the diagram, regardless of the criteria considered in the analysis. For application in base layers of flexible pavements [Figure 12a], the M3 mixture presented a desirability value close to 0.66. Moreover, the M3 mixture presented desirability values of 0.795 and 0.960, when applied in the subbase [Figure 13a] and subgrade reinforcement layers [Figure 14a], respectively. Since the M3 mixture presented the greatest desirability value, this mixture can be considered the most adequate construction material for the base, subbase and subgrade reinforcement layers of flexible pavements.

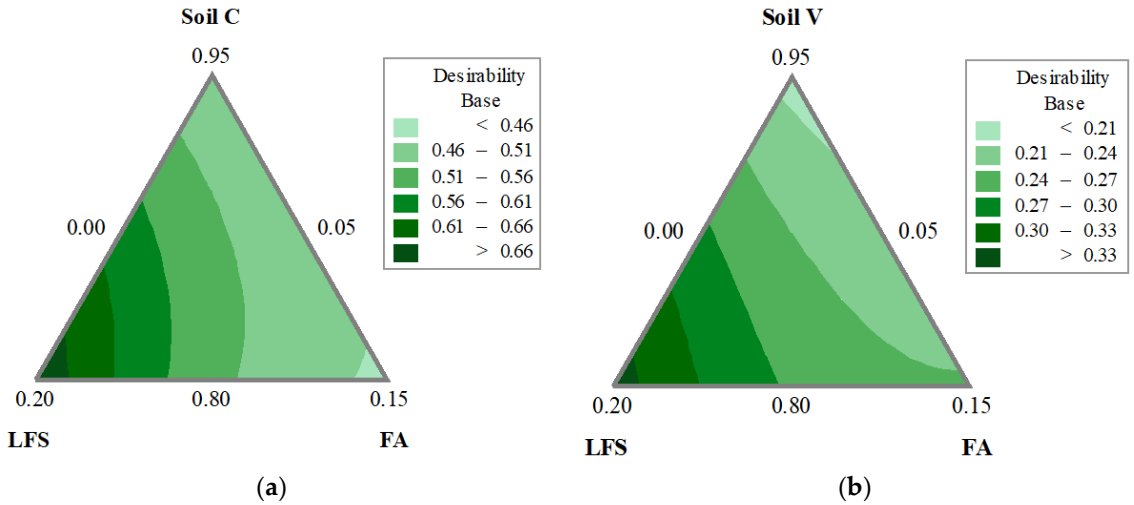

(**a**) (**b**)

Figure 12. Response surfaces regarding the desirability values of experimental mixtures prepared with Soil C (**a**) and V (**b**), considering their application as base course construction material.

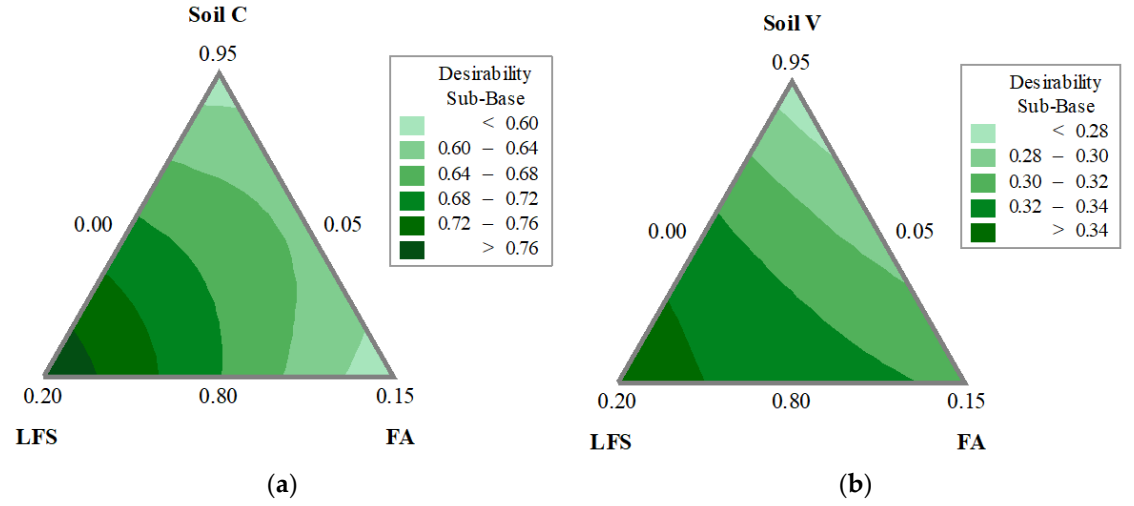

(**a**) (**b**)

Figure 13. Response surfaces regarding the desirability values of experimental mixtures prepared with Soil C (**a**) and V (**b**), considering their application as subbase course construction material.

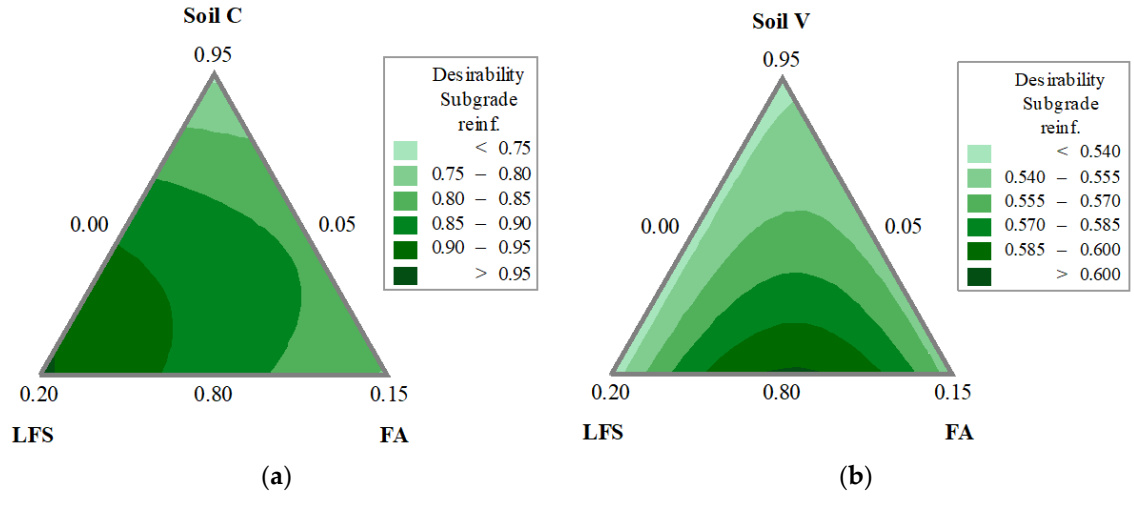

(**a**) (**b**)

Figure 14. Response surfaces regarding the desirability values of experimental mixtures prepared with Soil C (**a**) and V (**b**), considering their application as sub-ground reinforcement construction material.

For Soil V mixtures used in base and subbase applications [Figures 11b and 12b], the highest desirability values were verified for mixtures located at the left bottom corner of the diagram. With desirability values equal to 0.33 and 0.34 when considering criteria for application in base and subbase layers, respectively, the M3 mixture best met the criteria. Thus, it is possible to infer that this mixture presents the best performance when used in the construction of base and subbase layers of asphalt pavements. Regarding the application of the mixtures as subgrade reinforcement [Figure 14b], the desirability value increased towards the lower central edge of the diagram, so that the M4 mixture presented the highest desirability value (0.603). Therefore, the M4 mixture can be considered the most suitable material for the construction of subgrade reinforcement layers of asphalt pavements among the mixtures analyzed in the present work.

Since the M3 and M4 mixtures presented the highest desirability values among the mixtures analyzed in this research, they were able to concomitantly achieve the UCS-, CBR-, CBR-S- and RM-defined criteria and, therefore, can be considered mixtures with optimized performance. Although these mixtures presented the best performance, it is important to highlight that their desirability values were lower than 1.0, which indicates that they did not simultaneously meet all the technical criteria considered in this analysis.

5. Conclusions

This study presents original research on the concomitant use of LFS and FA as sustainable stabilizers for distinct soils, providing novel insights into their synergistic and antagonistic effects on the mechanical properties of pavement layers. The simplex-centroid methodology, desirability function, response surfaces and mathematical models revealed the mixture proportions of soil, LFS and FA that comply with pavement design regulations. The main conclusions obtained from this study are listed below:

- The addition of LFS and FA to the natural soils provided UCS, CBR index and RM increases up to 130.5%, 324.4% and 132.6%, respectively;
- LFS and FA generally provided higher mechanical properties improvements in sandy soils than in clayey soils;
- The use of industrial by-products caused small changes in the CBR-S of the natural soils, indicating that their application does not result in a significant increase in the expansion of the soil samples;
- The UCS, CBR and RM descriptive mathematical models showed R^2 values ranging from 0.760 to 0.998, which evidences the simplex-centroid accuracy in the description of these properties;
- The DoE methodology and the desirability function were useful for optimizing the mechanical properties, offering mixture proportions that meet the requirements established in the literature. The best proportions were 80% soil, 20% LFS and 0% FA for both soil samples;
- The comparison between estimated and actual values showed that the DoE was an effective tool for predicting and optimizing the properties of stabilized soils.

Future research should explore the interactions between other types of soils and sustainable stabilizer agents, using the DoE of mixtures in a simplex-centroid network. Examining the mechanical performance of sustainable materials for road construction, along with conducting comprehensive life cycle assessments (LCA), could unveil new strategies to enhance sustainability in the construction field. Future research should also explore the potential of incorporating LFS and FA into asphalt mixtures, offering additional insights into the development of sustainable and high-performance materials for pavement construction.

Author Contributions: Conceptualization, M.H.R.R., T.O.d.S., H.N.P., L.G.P., K.H.d.P.R., E.C.L. and G.H.N.; methodology, M.H.R.R.; validation, M.H.R.R.; formal analysis, M.H.R.R.; investigation, M.H.R.R.; resources, M.H.R.R.; data curation, M.H.R.R.; writing—original draft preparation, M.H.R.R.; writing—review and editing, M.H.R.R., T.O.d.S., H.N.P., L.G.P., K.H.d.P.R., E.C.L.

and G.H.N.; visualization, M.H.R.R.; supervision, T.O.d.S., H.N.P., L.G.P., K.H.d.P.R., E.C.L. and G.H.N.; project administration, T.O.d.S. All authors have read and agreed to the published version of the manuscript.

Funding: This study was financed in part by the Coordenação de Aperfeiçoamento de Pessoal de Nível Superior—Brasil (CAPES)—Finance Code 001.

Data Availability Statement: Data are contained within the article.

Acknowledgments: The authors would like to thank the support provided by CAPES and the Civil Engineering Department of the Federal University of Viçosa.

Conflicts of Interest: The authors declare no conflicts of interest.

References

1. Yildirim, I.Z.; Prezzi, M. Experimental evaluation of EAF ladle steel slag as a geo-fill material: Mineralogical, physical & mechanical properties. *Constr. Build. Mater.* **2017**, *154*, 23–33.
2. Bhatt, A.; Priyadarshini, S.; Acharath Mohanakrishnan, A.; Abri, A.; Sattler, M.; Techapaphawit, S. Physical, chemical, and geotechnical properties of coal fly ash: A global review. *Case Stud. Constr. Mater.* **2019**, *11*, e00263. [CrossRef]
3. Rodrigues, K.H.d.P.; Silva, T.O.d.; Pitanga, H.N.; Almeida, M.S.d.S.; Pedroti, L.G.; Rodrigues, M.H.R.; Lopes, E.C. Effect of carbonation of soil-slag mixtures on the resilient behaviour and structural response of an asphalt pavement. *Road Mater. Pavement Des.* **2024**, 1–20. [CrossRef]
4. Espinosa, A.B.; Revilla-Cuesta, V.; Skaf, M.; Serrano-López, R.; Ortega-López, V. Strength performance of low-bearing-capacity clayey soils stabilized with ladle furnace slag. *Environ. Sci. Pollut. Res.* **2023**, *30*, 101317–101342. [CrossRef] [PubMed]
5. Sahoo, S.; Prasad Singh, S. Strength and durability properties of expansive soil treated with geopolymer and conventional stabilizers. *Constr. Build. Mater.* **2022**, *328*, 127078. [CrossRef]
6. Rodrigues, K.H.d.P.; da Silva, T.O.; Pitanga, H.N.; Pedroti, L.G.; Rodrigues, M.H.R. Experimental study of mixtures soil-industrial waste using simplex design for application in paving. *J. Build. Eng.* **2023**, *78*, 107761. [CrossRef]
7. Lopes, E.C.; da Silva, T.O.; Pitanga, H.N.; Pedroti, L.G.; Franco de Carvalho, J.M.; Nalon, G.H.; de Lima, G.E.S.; de Araújo, E.N.D. Stabilisation of clayey and sandy soils with ladle furnace slag fines for road construction. *Road Mater. Pavement Des.* **2023**, *24*, 247–266. [CrossRef]
8. Islam, S.; Ara, S.; Islam, J. An experimental investigation on utilization of ladle refined furnace (LRF) slag in stabilizing clayey soil. *Heliyon* **2024**, *10*, e26004. [CrossRef]
9. Wang, H.; Liu, T.; Yan, C.; Wang, J. Expansive Soil Stabilization Using Alkali-Activated Fly Ash. *Processes* **2023**, *11*, 1550. [CrossRef]
10. Sengul, T.; Akray, N.; Vitosoglu, Y. Investigating the effects of stabilization carried out using fly ash and polypropylene fiber on the properties of highway clay soils. *Constr. Build. Mater.* **2023**, *400*, 132590. [CrossRef]
11. Espinosa, A.B.; López-Ausín, V.; Fiol, F.; Serrano-López, R.; Ortega-López, V. Analysis of the deformational behavior of a clayey foundation soil stabilized with ladle furnace slag (LFS) using a finite element software. *Mater. Today Proc.* 2023, *in press*. [CrossRef]
12. Abdila, S.R.; Abdullah, M.M.A.B.; Ahmad, R.; Burduhos Nergis, D.D.; Rahim, S.Z.A.; Omar, M.F.; Sandu, A.V.; Vizureanu, P.; Syafwandi. Potential of Soil Stabilization Using Ground Granulated Blast Furnace Slag (GGBFS) and Fly Ash via Geopolymerization Method: A Review. *Materials* **2022**, *15*, 375. [CrossRef] [PubMed]
13. Fathonah, W.; Intari, D.E.; Mina, E.; Kusuma, R.I.; Mahfudoh. Stabilization of clay using slag and fly ash with reference to UCT value (Case study: Jalan Kadusentar, Pandeglang District-Banten). In Proceedings of the IOP Conference Series: Materials Science and Engineering, Bali, Indonesia, 7–8 August 2019; Volume 673, p. 012038.
14. Mina, E.; Kusuma, R.I.; Ulfah, N. Utilization of steel slag and fly ash in soil stabilization and their effect to california bearing ratio (CBR) value. (Case study: Kp. Kadusentar road Medong village Mekarjaya Subdistrict Pandeglang District). In Proceedings of the IOP Conference Series: Materials Science and Engineering, Bali, Indonesia, 7–8 August 2019; Volume 673, p. 012034.
15. Pitanga, H.N.; Silva, T.O.d.; Santos, A.L.d.; Silva, A.C.B.; Lima, D.C.d. MCT classification for compacted mixtures of soil-steel slag-fly ash for application in forest roads. *Rev. Árvore* **2016**, *40*, 911–919. [CrossRef]
16. Rajakumaran, K. An experimental analysis on stabilization of expansive soil with steel slag and fly ash. *Int. J. Adv. Eng. Technol.* **2015**, *7*, 1745.
17. Soyonar, E.; Fırat, S.; Yilmaz, G.; Okur, V. *Performance of Steel Slag and Fly Ash Added Soil as Subbase Materials*; Springer International Publishing: Cham, Switzerland, 2018; pp. 799–807.
18. Wang, G.; Wang, Y.; Gao, Z. Use of steel slag as a granular material: Volume expansion prediction and usability criteria. *J. Hazard. Mater.* **2010**, *184*, 555–560. [CrossRef] [PubMed]
19. Montgomery, D.C. *Design and Analysis of Experiments*; John Wiley & Sons: Hoboken, NJ, USA, 2017.
20. Jiao, D.; Shi, C.; Yuan, Q.; An, X.; Liu, Y. Mixture design of concrete using simplex centroid design method. *Cem. Concr. Compos.* **2018**, *89*, 76–88. [CrossRef]
21. Wu, J.; Liu, Q.; Deng, Y.; Yu, X.; Feng, Q.; Yan, C. Expansive soil modified by waste steel slag and its application in subbase layer of highways. *Soils Found.* **2019**, *59*, 955–965. [CrossRef]

22. Medeiros, V.S.C.; Pedroti, L.G.; Mendes, B.C.; Pitanga, H.N.; Silva, T.O.d. Study of mixtures using simplex design for the addition of chamotte in clay bricks. *Int. J. Appl. Ceram. Technol.* **2019**, *16*, 2349–2361. [CrossRef]
23. Mendes, B.C.; Pedroti, L.G.; Fontes, M.P.F.; Ribeiro, J.C.L.; Vieira, C.M.F.; Pacheco, A.A.; Azevedo, A.R.G.d. Technical and environmental assessment of the incorporation of iron ore tailings in construction clay bricks. *Constr. Build. Mater.* **2019**, *227*, 116669. [CrossRef]
24. Iwański, M.; Buczyński, P.; Mazurek, G. Optimization of the road binder used in the base layer in the road construction. *Constr. Build. Mater.* **2016**, *125*, 1044–1054. [CrossRef]
25. Onyelowe, K.; Alaneme, G.; Igboayaka, C.; Orji, F.; Ugwuanyi, H.; Bui Van, D.; Nguyen Van, M. Scheffe optimization of swelling, California bearing ratio, compressive strength, and durability potentials of quarry dust stabilized soft clay soil. *Mater. Sci. Energy Technol.* **2019**, *2*, 67–77. [CrossRef]
26. *ABNT NBR 7181*; Soil—Grain Size Analysis. Associação Brasileira de Normas Técnicas: Rio de Janeiro, Brazil, 2016; p. 12.
27. *ABNT NBR 6458*; Gravel Grains Retained on the 4.8 mm Mesh Sieve—Determination of the Bulk Specific Gravity, of the Apparent Specific Gravity and of Water Absorption. Associação Brasileira de Normas Técnicas: Rio de Janeiro, Brazil, 2016; p. 10.
28. *ABNT NBR 6459*; Soil—Liquid Limit Determination. Associação Brasileira de Normas Técnicas: Rio de Janeiro, Brazil, 2016; p. 5.
29. *ABNT NBR 7180*; Soil—Plasticity Limit Determination. Associação Brasileira de Normas Técnicas: Rio de Janeiro, Brazil, 2016; p. 3.
30. Manso, J.M.; Ortega-López, V.; Polanco, J.A.; Setién, J. The use of ladle furnace slag in soil stabilization. *Constr. Build. Mater.* **2013**, *40*, 126–134. [CrossRef]
31. Akinwumi, I. Soil Modification by the Application of Steel Slag. *Period. Polytech. Civ. Eng.* **2014**, *58*, 371–377. [CrossRef]
32. Mahmudi, M.; Altun, S.; Eskisar, T. Experimental and Numerical Evaluation of Clay Soils Stabilized with Electric Arc Furnace (EAF) Slag. *Adv. Sustain. Constr. Resour. Manag.* **2021**, *144*, 73.
33. *ABNT NBR 12653*; Pozzolanic Materials—Requirements. Associação Brasileira de Normas Técnicas: Rio de Janeiro, Brazil, 2014.
34. *ISO 13320 2020*; Particle Size Analysis—Laser Diffraction Methods. International Organization for Standardization: Genève, Switzerland, 2020.
35. *ABNT NBR 16372*; Portland Cement and Other Powdered Materials—Determination of Fineness by the Air Permeability Method (Blaine Method). Associação Brasileira de Normas Técnicas: Rio de Janeiro, Brazil, 2019.
36. *ABNT NBR 11579*; Portland Cement—Determination of Fineness Index by Means of the 75 µm Sieve (nº 200). Associação Brasileira de Normas Técnicas: Rio de Janeiro, Brazil, 2012.
37. *ABNT NBR 16605*; Portland Cement and Other Powdered Material—Determination of the Specific Gravity. Associação Brasileira de Normas Técnicas: Rio de Janeiro, Brazil, 2017.
38. Lopes, M.M.S.; Alvarenga, R.d.C.S.S.A.; Pedroti, L.G.; Ribeiro, J.C.L.; de Carvalho, A.F.; Cardoso, F.d.P.; Mendes, B.C. Influence of the incorporation of granite waste on the hiding power and abrasion resistance of soil pigment-based paints. *Constr. Build. Mater.* **2019**, *205*, 463–474. [CrossRef]
39. Bin-Shafique, S.; Rahman, K.; Yaykiran, M.; Azfar, I. The long-term performance of two fly ash stabilized fine-grained soil subbases. *Resour. Conserv. Recycl.* **2010**, *54*, 666–672. [CrossRef]
40. Jha, A.K.; Sivapullaiah, P.V. Mechanism of improvement in the strength and volume change behavior of lime stabilized soil. *Eng. Geol.* **2015**, *198*, 53–64. [CrossRef]
41. Ortega-López, V.; Manso, J.M.; Cuesta, I.I.; González, J.J. The long-term accelerated expansion of various ladle-furnace basic slags and their soil-stabilization applications. *Constr. Build. Mater.* **2014**, *68*, 455–464. [CrossRef]
42. *ABNT NBR 12025*; Soil—Cement—Simple Compression Test of Cylindrical Specimens—Method of Test. Associação Brasileira de Normas Técnicas: Rio de Janeiro, Brazil, 2012.
43. *ABNT NBR 9895*; Soil—California Bearing Ratio (CBR)—Testing Method. Associação Brasileira de Normas Técnicas: Rio de Janeiro, Brazil, 2016.
44. *DNIT ME 134*; Paving—Soils—Resilient Modulus Determination—Testing Method. Departamento Nacional de Infraestrutura de Transportes: Rio de Janeiro, Brazil, 2018.
45. *ABNT NBR 12253*; Soil-Cement—Mixture for Use in Pavement Layer—Procedure. Associação Brasileira de Normas Técnicas: Rio de Janeiro, Brazil, 2012.
46. Nega, A.; Nikraz, H. Evaluation of Tire-Pavement Contact Stress Distribution of Pavement Response and Some Effects on the Flexible Pavements. In *Airfield and Highway Pavements.*; ASCE: Philadelphia, PA, USA, 2017; pp. 174–185.
47. Islam, M.R.; Tarefder, R.A. *Pavement Design: Materials, Analysis, and Highways*; McGraw-Hill Education: New York, NY, USA, 2020.
48. Franco, F.A.C.d.P.; Motta, L.M.G.d. *Manual para Utilização do Método Mecanístico-Empírico MeDiNa*; Departamento Nacional de Infraestrutura de Transportes: Rio de Janeiro, Brazil, 2020; p. 78.
49. Pezo, R.F.; Claros, G.; Hudson, W.R.; Stokoe, K.H., II. *Development of a Reliable Resilient Modulus Test for Subgrade and Non-Granular Subbase Materials for Use in Routine Pavement Design*; The University of Texas at Austin: Austin, TX, USA, 1992.
50. *DNIT IS-247*; Studies for Elaboration of Implementation Projects Using the National DesignMethod—MeDiNa. Departamento Nacional de Infraestrutura de Transportes: Rio de Janeiro, Brazil, 2021.
51. *AASHTO T220-66 (2013)*; Standard Method of Test for Determination of the Strength of Soil-Lime Mixtures. American Association of State and Highway Transportation Officials: Washington, DC, USA, 2018.

52. Ardah, A.; Chen, Q.; Abu-Farsakh, M. Evaluating the performance of very weak subgrade soils treated/stabilized with cementitious materials for sustainable pavements. *Transp. Geotech.* **2017**, *11*, 107–119. [CrossRef]
53. DNIT. *Manual de Pavimentação*; Departamento Nacional de Infraestrutura de Transportes: Rio de Janeiro, Brazil, 2006; p. 274.
54. AASHTO. *Mechanistic-Empirical Pavement Design Guide: A Manual of Practice*, 3rd ed.; American Association of State Highway and Transportation Officials: Washington, DC, USA, 2020.
55. Abo-Shanab, Z.; Ragab, A.; Naguib, H. Improved dynamic mechanical properties of sustainable bio-modified asphalt using agriculture waste. *Int. J. Pavement Eng.* **2019**, *22*, 905–911. [CrossRef]
56. Bhuvaneshwari, S.; Robinson, R.; Gandhi, S. Resilient modulus of lime treated expansive soil. *Geotech. Geol. Eng.* **2019**, *37*, 305–315. [CrossRef]
57. Sebbar, N.; Lahmili, A.; Bahi, L.; Ouadif, L. Treatment of Clay Soils with Steel Slag, in Road Engineering. In *E3S Web of Conferences*; EDP Sciences: Ulysse, France, 2020; p. 02017.
58. Hou, G.; Yan, Z.; Sun, J.; Naguib, H.; Lu, B.; Zhang, Z. Microstructure and mechanical properties of CO_2-cured steel slag brick in pilot-scale. *Constr. Build. Mater.* **2021**, *271*, 121581. [CrossRef]
59. Lopes, E.C.; da Silva, T.O.; Pitanga, H.N.; Pedroti, L.G.; Franco de Carvalho, J.M.; Nalon, G.H.; Lima, G.E.S.d.; Rodrigues, M.H.R. Application of electric arc furnace slag for stabilisation of different tropical soils. *Int. J. Pavement Eng.* **2022**, *23*, 5003–5014. [CrossRef]
60. Rezende, J. Study of Mixtures of Soil and Steel Waste Statistically Optimized for Applications in Landfill Liners. Ph.D. Thesis, Federal University of Viçosa, Viçosa, Brazil, 2024; *in press*.
61. *ABNT NBR 10004*; Solid Waste—Classification. Associação Brasileira de Normas Técnicas: Rio de Janeiro, Brazil, 2004.
62. Skels, P.; Haritonovs, V.; Pavlovskis, E. Wood fly ash stabilized road base layers with high recycled asphalt pavement content. *Balt. J. Road Bridge Eng.* **2021**, *16*, 1–15. [CrossRef]